

# MAROC Sum readout for HA12700-03 MaPMT

Bishnu Karki\*, Zhiwen Zhao\*, Bo Yu\*, Drew Smith\*, Haiyan Gao\*, Benjamin Raydo\*\*, and Alexandre Camsonne\*\*

Duke University\*

Thomas Jefferson National Accelerator Facility\*\*

(Dated: January 10, 2025)

## CONTENTS

I. Introduction	1
II. FADC Signal Oscillation	2
III. Saturation study of MAROC sum board	2
A. Pixel TDC threshold study	3
IV. High rate Benchtest	4
V. Ring test	5
A. LED Ring Analysis	8
B. Cosmic Test	10
VI. Conclusion	12
References	13

## I. INTRODUCTION

To maximize the science return of the 12 GeV upgrade of the Thomas Jefferson Accelerator Facility (TJNAF, a.k.a Jefferson Lab or JLab) the Solenoidal Large Intensity Device (SoLID) [1] is proposed to be built in the experimental Hall A. SoLID will have full  $2\pi$  azimuthal coverage and can handle high luminosity. JLab Program Advisory Committee (PAC) has already approved several experiments [2–6] that will be using the SoLID. The SoLID will use the Cherenkov detector for particle identification. The Cherenkov detector rate is expected as high as 200kHz/pixel (pixel size of  $6 \times 6 \text{ mm}^2$ ) in most of the approved experiments. In order to handle such a high rate, we need to have compatible readout electronics for the photosensors. The study by Peng *et al.* [7] showed that the commercially available Multi-anode Photomultipliers (MaPMTs) with JLab FADC250 modules were able to operate in a high background rate environment similar to SoLID. In their study, they used a simple sum readout that had 4 output channels for a MaPMT. Each channel gave the sum of charge collected in a group of 16 pixels, a quadrant of a MaPMT. On the other hand, the CLAS12 RICH detector has used Multi-Anode Readout Chip (MAROC) electronics [8] to have TDC signals from 64 pixels of a MaPMT. The CLAS12 RICH validated the performance of MAROC readout up to 2 kHz/pixel [9] which is almost two orders of magnitude smaller than the rate expected in SoLID.

MAROC readout includes an adaptor board to hold up to 3 MaPMTs, an ASIC board hosting MAROC chips, and FPGA board with optical fibers to communicate with the Subsystem Processor (SSP) module in Data Acquisition (DAQ) to record TDC signals from 64 pixels of each MaPMT. For SoLID Cherenkov detectors, to allow collecting pixel information and provide trigger with the sum of photons on pixels simultaneously, the new MAROC sum electronics were designed and manufactured in collaboration with the INFN Ferrara group and the JLab fast electronic group. By inserting a new sum board between a modified ASIC board and an FPGA board, charges in pixels are summed and separated into four quadrant sums and one total sum. A newly designed converter board then transfers the sum

signals to communicate with JLab flash ADC boards in DAQ. The photos in Fig. 1 show the five boards mentioned above and how they are connected together to form the MAROC sum electronics. In this paper, we will discuss the feature and performance of the MAROC sum electronics which has not been used before.

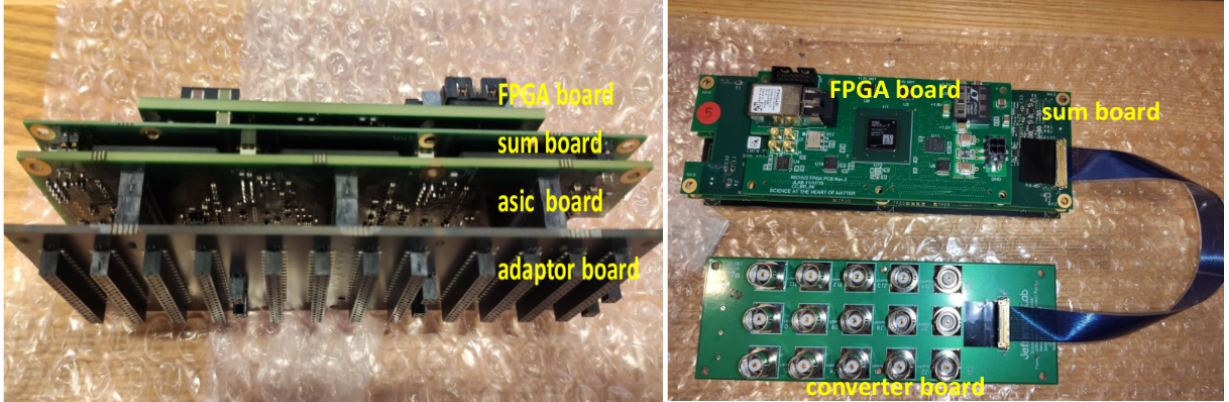


FIG. 1. Photos of the MAROC sum boards, including adaptor, ASIC, sum, FPGA, and converter boards, are shown. The ASIC board is modified from its original version to accommodate the new sum board. A newly made converter board connects the new sum board output to regular BNC connectors through an I-PEX cable.

## II. FADC SIGNAL OSCILLATION

The sum and FPGA board in each set of MAROC sum board are powered by low voltage (LV) with single cable. When multiple MAROC sum boards are powered at once we observed a huge pedestal oscillation in both quad and total sum signals. However, oscillation was not observed when single MAROC sum board was used to read a MaPMT. The oscillation was from sum board due to the coupling of LV between boards. To mitigate the issue MAROC sum board was modified with help of the JLab fast electronics group. First, the LV connector to FPGA and sum board was separated then a voltage regulator was added to the sum board. These modifications helped to reduce the pedestal width by a factor of 5. Fig. 2 shows the width of the pedestal before (purple) and after (green) modifications compared with pedestal when single MAROC board in operation (red). With the modification of the sum board, we achieved the width of the pedestal comparable to one we had while operating single set of MAROC board. One caveat of the modification of sum board was the increment in the FADC signal width to 40 ns which is almost a factor of 2 larger as compared to one before modification. We are discussing with JLab electronics group to find the possible way to minimize the FADC signal window which will be helpful to reduce the background entering in signal window.

## III. SATURATION STUDY OF MAROC SUM BOARD

In addition to the TDC information from pixels of MaPMT, the MAROC sum electronics provides an analog sum of charge collected in a group of pixels. MAROC sum board sums the charge collected in a group of 8 pixels to provide a total of 8 analog sums as shown in Fig. 3 (Top). For a quadrant signal, two sums each of 8 pixels are added and for the total sum, all 8 sums are added. For instance, quadrant 1 is the sum of “SUM1” and “SUM2”. The output analog sum should be linear to the amount of charge injected. But if the injected charge is large enough then the MAROC sum starts saturating i.e the output signal won’t be linear to injected charge. We carried out a study to determine the maximum number of photoelectrons that a single pixel, quadrant, and the sum signal can hold before saturation. For our test, we injected the known charge in a given pixel or group of pixels in an increasing step and recorded the MAROC sum output.

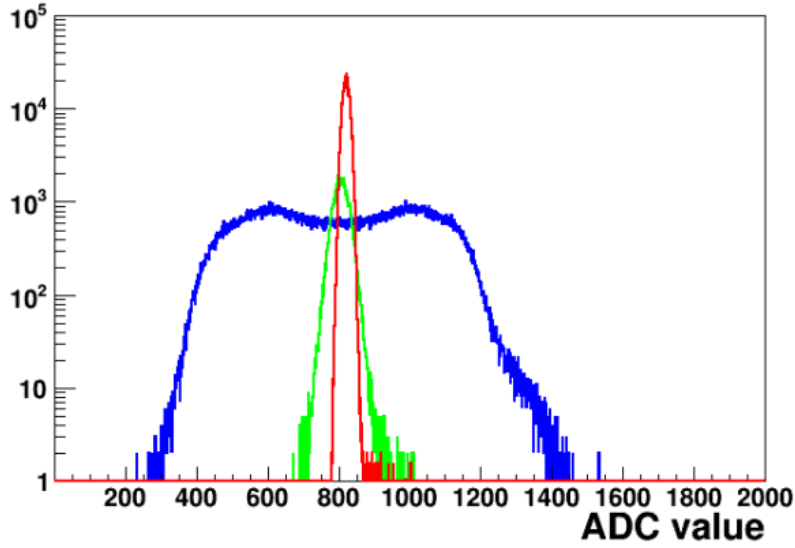


FIG. 2. Comparison of the total sum FADC pedestal before and after the modification of the boards. The red histogram is with one set in use. The blue and green histograms are with 5 MAROC board powered at once before and after the modification of the sum board respectively.

Fig. 4 shows the number of photoelectrons (corresponding to MaPMT at 850 V) for different injected charges with only one pixel fired. The red line is a linear fit to the data. The blue vertical and horizontal dashed lines represent the threshold charge in the DAC unit and the number of photoelectrons respectively above which the sum signal saturates. Using the measured value of the position of the mean peak of a Single Photoelectron (SPE) distribution the ADC value is converted to a number of photoelectrons (NPE) that a pixel can withstand before saturation. The saturation limit varies with the number of pixels fired in a group of 8 pixels shown in Fig. 3. Table I shows the maximum number of photoelectrons for an individual pixel, quadrant, and total sum below which the MAROC sum is linear to the injected charge. We performed our study by applying different HV to MaPMT and found that the linear range decrease with an increase in HV.

	Number of pixels fired		
HV (V)	1 pixel	16 pixels (Quad)	64 pixels (Total Sum)
850	3	10	44
900	2	7	29
1000	1	4	17

TABLE I. Saturation limit for the MAROC sum board in terms of NPE for a single pixel, quad, and total sum signal at different high voltage for MaPMT. With the increment in HV applied to MaPMT the linear dynamic range gets reduced.

#### A. Pixel TDC threshold study

For MAROC pixel readout like in CLAS12 RICH, MaPMTs are usually operated at around 1000 V. But to have both pixel and ADC readout at once we found that one can get benefit of larger linear region while operating MaPMT at lower voltage. To find the optimized value of the TDC threshold at 850 V, we plotted the duration of a hit at

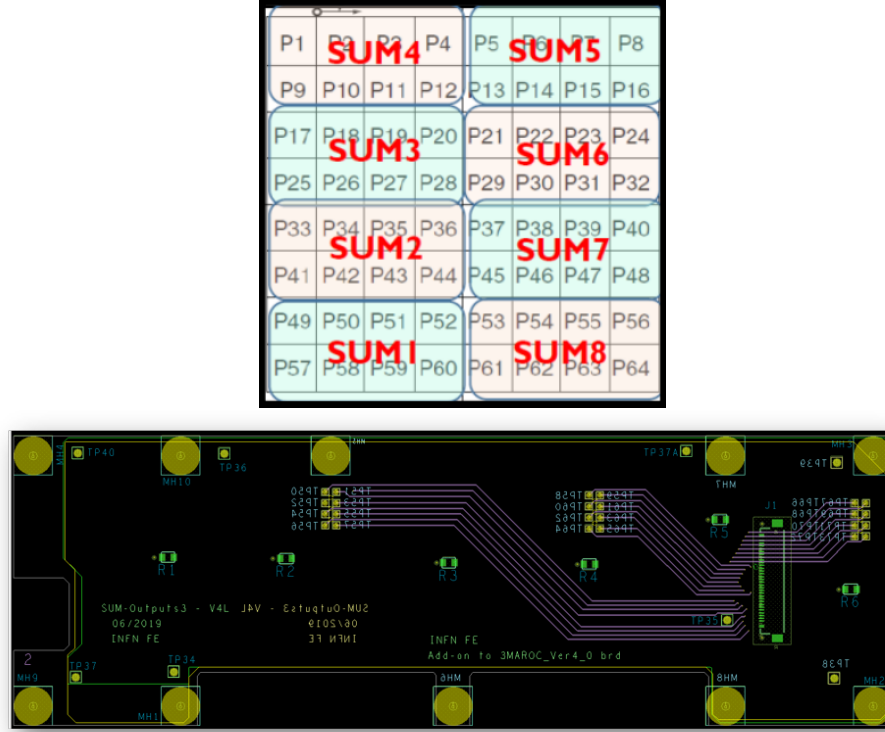


FIG. 3. Top: The schematic representation of the summing mechanism of MAROC sum board for H12700 MaPMT series with 64 pixels. MAROC sum board sums group of 8 pixels. The “SUM1” and “SUM2”) give first quadrant signal, “SUM3” and “SUM4” give the second quadrant, and so on. The total sum represents the sum of charge collected in all 64 pixels coming from 8 sums. Bottom: The sum board design.

different TDC thresholds. The duration of a hit is defined as the difference in time when the trailing and leading edge cross the TDC threshold. The duration of a hit depends on the amplitude of a signal. For cross-talk (small amplitude) the duration of a hit is small compared to the signal. Fig. 5 shows the duration of hit distribution for 3 typical TDC discriminator threshold values 10, 30, and 50 DAC units above the average pedestal value. At the lower threshold, we record a lot of lower amplitude noise and at the higher threshold, we may miss a small amplitude signal. After these tests, the common discriminator threshold was set to +30 DAC units above the average MaPMT pedestal position, a level that corresponds to a small fraction of the average SPE amplitude. To make sure that our choice of TDC threshold does not reject the SPE signal we compared the number of photoelectrons distributions for two identical runs with the same TDC threshold, +30 above the mean pedestal. The red and the blue distribution in Fig. 6 corresponds to MaPMT at 1000 V and 850 V respectively. The mean of the NPE distribution at 850 V is about 95% of the distribution at 1000 V. It suggests that MaPMT at 850 V, TDC threshold of +30 DAC units above the mean pedestal is sufficient to record the small-amplitude signal with minimal loss of efficiency.

#### IV. HIGH RATE BENCHTEST

One of our goal was to test the performance of MAROC sum electronics up to the maximum expected SoLID rates, 200 kHz/pixel for pixel readout or 4 MHz/PMT (MaPMT size  $5 \times 5 \text{ cm}^2$ ) for sum readout. Due to lack of beam time we performed our test at bench using Light Emitting Diodes (LEDs) and a laser as light sources. The schematic layout for the bench test is shown in Figure 7. Pulsed laser (470 nm) was used as signal and a LED (275 nm) operated with DC voltage was used to mimic the background. The amount of light from the LED was controlled by changing

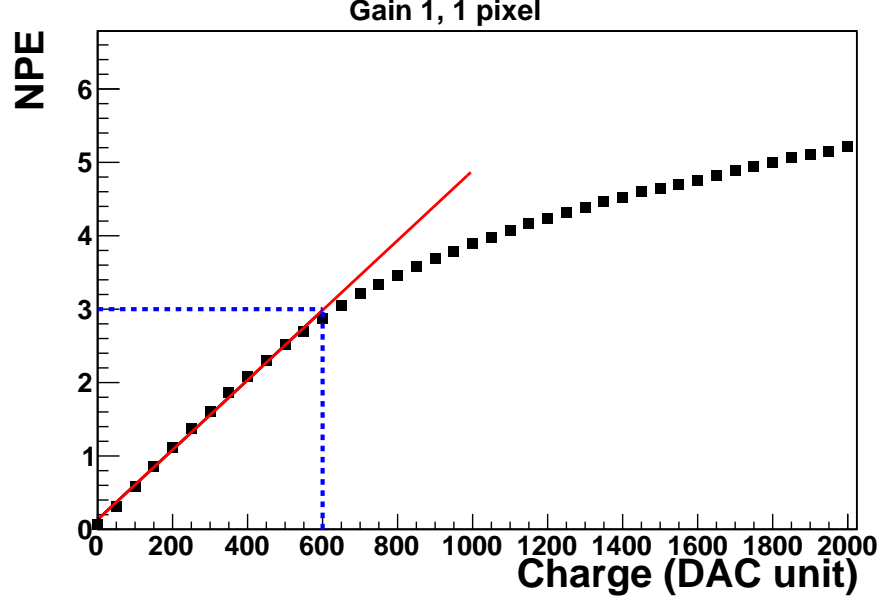


FIG. 4. Saturation study of MAROC sum board with one pixel fired. The number of photoelectrons vs injected charge in DAC unit. The red line is a linear fit to the data. The maximum value of charge injected and the number of photoelectrons before saturation is shown by the dashed blue vertical and horizontal lines for MaPMT at 850 V.

the applied DC voltage. The filter (diffuser) placed in between the laser source and MaPMT was changed to choose different laser light intensities: strong, medium, and weak laser light. Light from LED and laser was collected by a Hamamatsu H12700-03 series MaPMT with MAROC sum readout. MAROC output had two independent pieces of information: TDC signal from 64 pixels and 5 FADC sum signals including 4 quads of 16 pixels each and 1 sum of 64 pixels. An independent pulse generator (clock) synchronized with laser was used as a random trigger.

We used LED operated in DC voltage and pulsed laser to achieve the high rate in our photosensor. To ensure the desired rate was achieved, we measured the scaler rate for both readouts FADC and pixel scaler. In the case of TDC, the single event may result in multiple pixel hits but the FADC sums as a single event. The two scalers: pixel scaler and sum scaler rate can be related using Equation 1.

$$\text{Sum scaler rate} = \frac{\text{Average pixel scaler rate} \times 64}{\text{Average pixel occupancy}} \quad (1)$$

where average pixel scaler rate is an average hit of 64 pixels and the average pixel occupancy is an average number of pixel hits for an event. Fig. 8 shows the agreement between the rates from the sum scaler and pixel scaler for LED operating at different DC voltage is within 3%. With LED operating in DC, we achieved the background rate  $\sim 6$  MHz/PMT, 50% larger than expected in SoLID.

For the given signal we have two independent information coming from pixel and FADC readout. If the electronics is performing well at high rate then one should expect the linear correlation between these two readouts. We found the linear correlation between the TDC and FADC signal as shown in Fig. 9 up to the sum rate  $\sim 6$  MHz/PMT. This demonstrates that summing electronics work as expected to collect the charge from pixels.

## V. RING TEST

In the Cherenkov detector, the Cherenkov ring is analyzed for particle identification. To study the performance of MAROC sum electronics and the efficiency of our algorithms we analyzed the ring formed at MaPMT in presence of

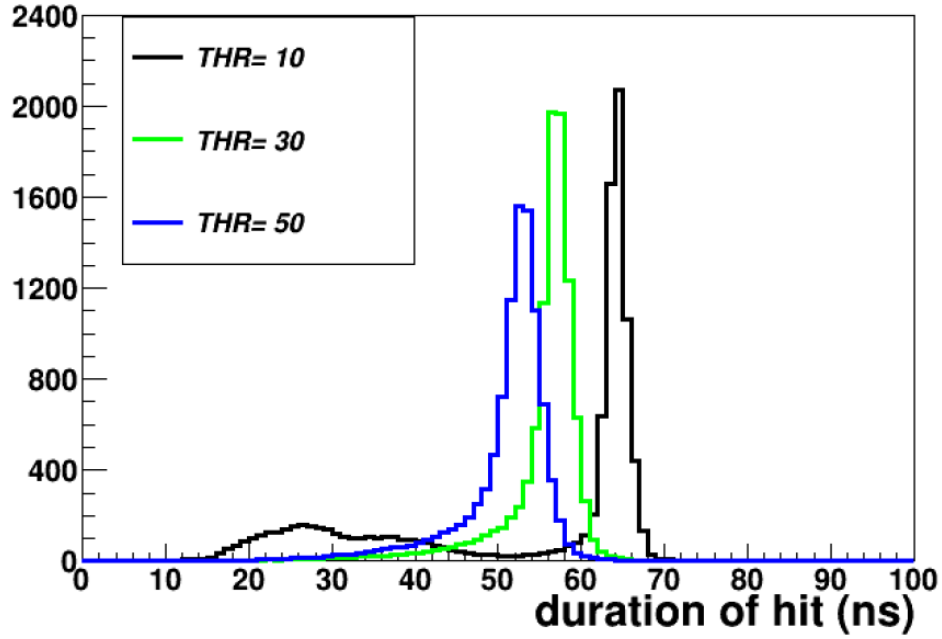


FIG. 5. Duration of hit distribution from pixel readout of the MAROC sum board at 3 different values of thresholds 10, 30, and 50 DAC units above the average pedestal position, with MAPMT at 850 V.

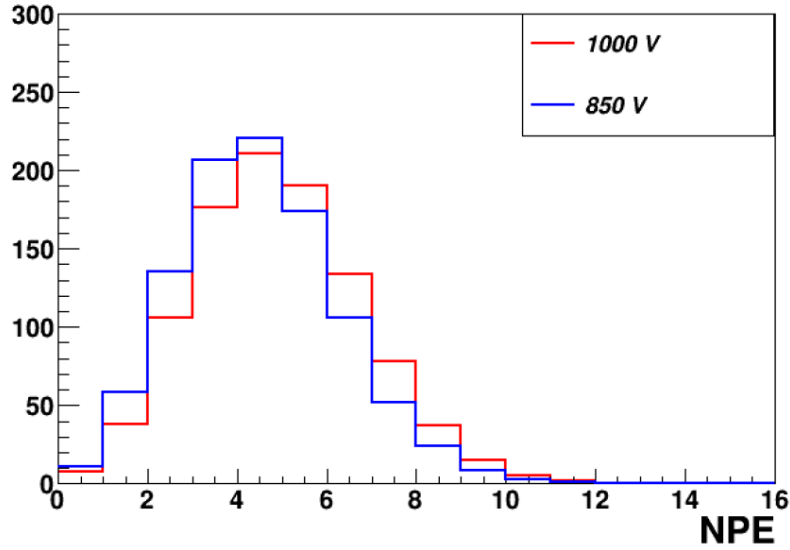


FIG. 6. A number of photoelectrons (NPE) distribution with TDC threshold +30 DAC unit above pedestal for two identical settings. The NPE distribution with MaPMT at 1000V is represented by the red histogram while the blue histogram is for MaPMT at 850 V.

background comparable to SoLID running condition. On our setup the background was generated by LED operated by DC voltage. We had two setups for producing the rings, one using the LED to produce ring on photosensors and another using the cosmic muon to produce the real Cherenkov photons on photosensors. We analyzed these ring for both pixel and sum readout using two algorithms:

- Number of photoelectron cuts which is most straightforward

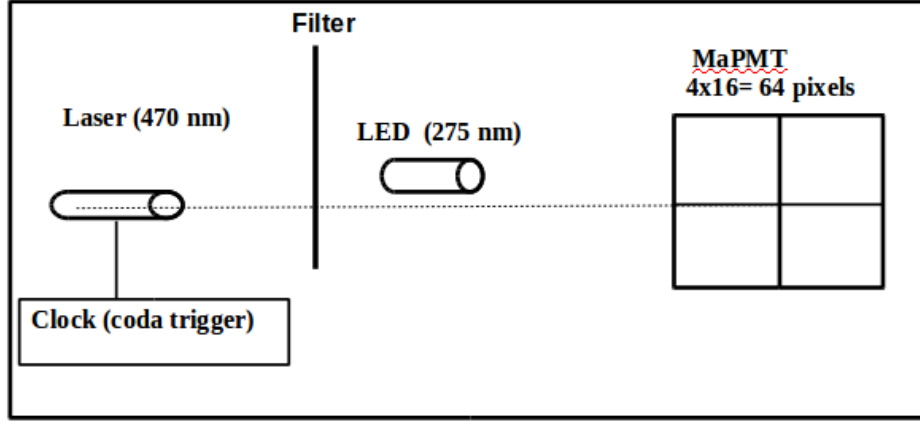


FIG. 7. Schematic layout of bench test set up. The entire setup was placed inside the black box to minimize the background.

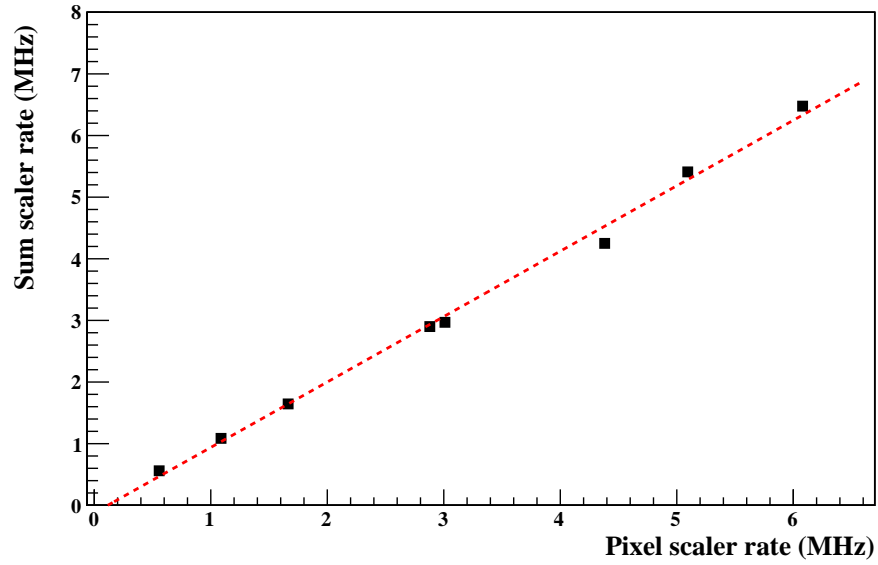


FIG. 8. Comparison between the sum and pixel scaler rates. The agreement between the two scaler rates are within 3% for rates similar to that expected in SoLID.

- Hough circular transform, the ring finder algorithm from computer vision

To test the performance our algorithm we defined the term accuracy or Figure of Merit (FOM) for accepting signal and rejecting background as in Eq.1 2 and Eq. 3 respectively. The ideal result would have both FOMs' as large as possible or at least larger than 90%.

$$(Accuracy/FOM)_{signal} = \frac{\text{number of accepted signal events}}{\text{total signal events}} \quad (2)$$

$$(Accuracy/FOM)_{background} = \frac{\text{number of rejected background events}}{\text{total background events}} \quad (3)$$

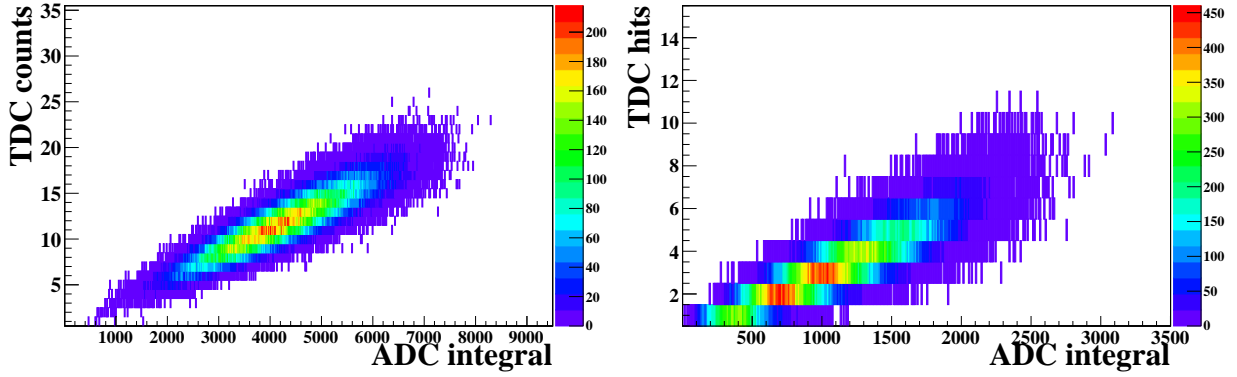


FIG. 9. Left: TDC counts VS ADC total sum signal. Right: TDC counts vs ADC one quadrant sum signal. The linear correlation between pixel signals read-out by MAROC TDCs and sum signals read-out by flash ADCs is observed from the MaPMT with MAROC sum readout tested with LED.

#### A. LED Ring Analysis

Two similar LEDs (275 nm) were enclosed inside a box. The pulsed light from the first LED was passed through the circular filter to form a ring near the center of the MaPMT array with a radius close to 8 pixels. The second LED was operated with DC voltage to provide continuous background. The background level from the second LED was controlled by adjusting the voltage of its DC power supply. Fig. 10 shows the schematic experimental setup to produce the LED rings. We collected the data at a different level of background up to almost twice as expected in the SoLID running condition. Position and ring size are fixed for the LED ring so they are relatively simple to identify from the background. But still helps us to test the performance of our algorithm.

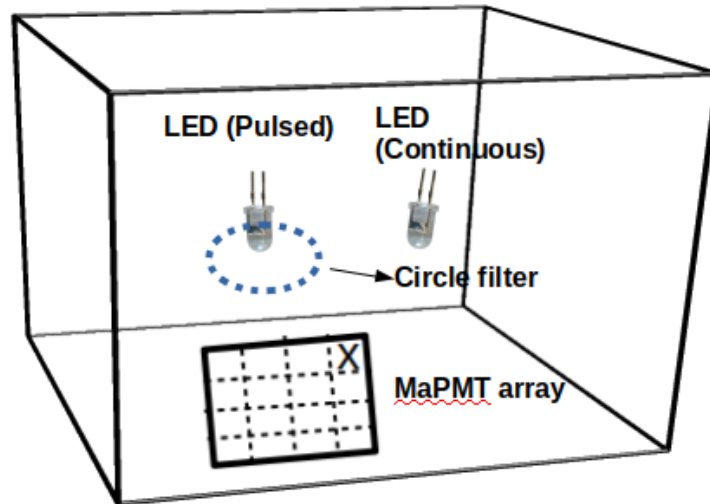


FIG. 10. Schematic layout for LED ring. For signal, we used pulsed LED. Light from the pulsed LED is passed through the circular filter before it is collected in the MaPMTs array, 15 MaPMTs shown by the grid. The second LED operated with DC voltage provides the background. The entire setup was placed inside the black box to avoid any external light.

Fig. 11 shows at the lower background level, less than 200 kHz/pixel, the background distribution is well separated from the signal in presence of background. At these lower background rates, the simple number of photoelectron cuts is sufficient enough to separate the signal from a background with better than 90% accuracy. But at a higher



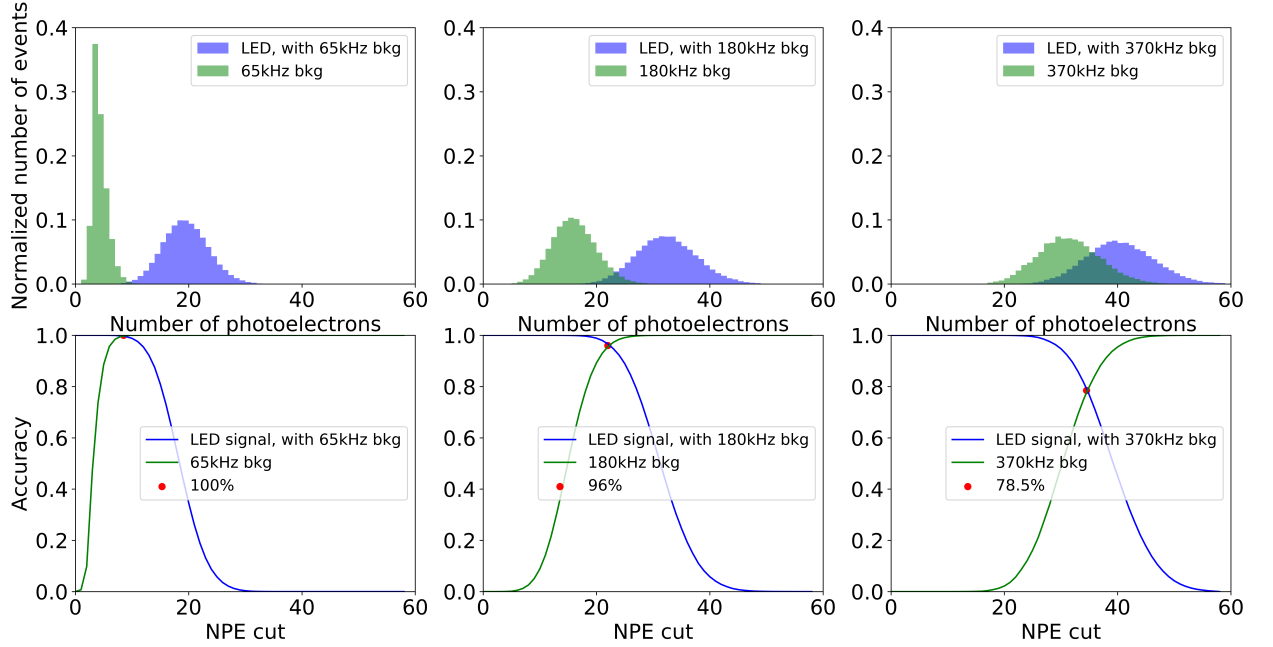


FIG. 11. Top: Number of photoelectron distribution for LED ring with pixel readout. The green and the purple histogram represents a number of photoelectrons with background only and LED signal in presence of background. The histograms are at the background rate of 65, 180, and 370 kHz/pixel from left to right. Bottom: The figure of merit for the number of photoelectrons cut at different levels of background.

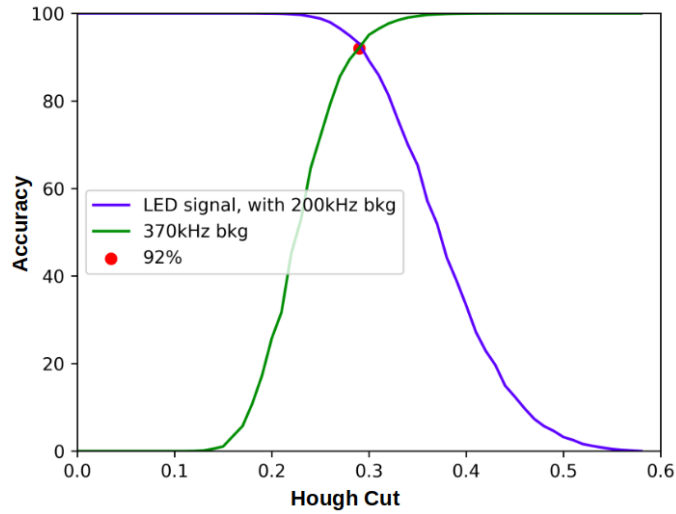


FIG. 12. The figure of merit for the Hough transformation algorithm at background of 370 kHz/pixel. At high background environment the Hough transformation performs well compared to number of photoelectron cut.

background rate, the background and signal (in presence of background) distribution are more overlapped and the number of photoelectron cuts is not sufficient enough to reject the background from the signal. At higher background the more complicated Hough transform algorithm is used. Fig. 12 demonstrates with Hough transformation, the accuracy is improved from 70% to 92% at the random background of 370 kHz/pixel. The parameters of the recognized

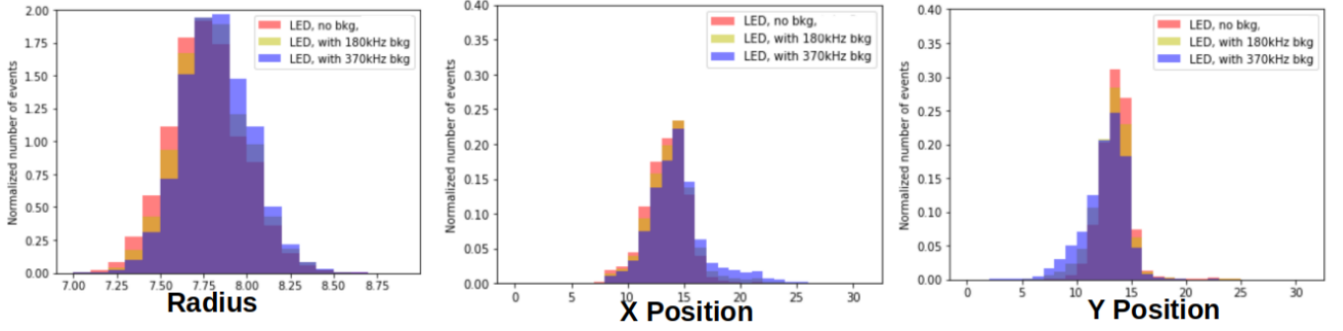


FIG. 13. Parameters of the recognized rings using the Hough transformation for pixel readout. The reconstructed radius and position of the ring are in agreement with the experimental setup.

rings were reconstructed using Hough transformation. Fig. 13 shows the reconstructed parameters of ring: radius, X, and Y positions of the LED ring at various background rates. The reconstructed parameters are in good agreement with the experimental setup.

We also analyzed the sum readout results for the same LED ring data. The quad sum readout using Hough transformation method can provide similar separation with larger uncertainty than the pixel readout. It's much more difficult for total sum readout to use Hough transformation method because the ring only covers about 4 PMTs.

## B. Cosmic Test

We also tested the Cherenkov ring produced using the cosmic muon. Figure 14 shows the schematic layout for the cosmic ring test. As the cosmic muon passes through the 4 cm lucite radiator, refractive index of 1.5, the Cherenkov light is emitted then collected in 15 MaPMTs array. The opening angle of Cherenkov light ( $48.2^\circ$ ) is larger than the critical angle of lucite for total internal reflection ( $41.8^\circ$ ). As a consequence, the Cherenkov light emitted with vertical cosmic muon won't be able to pass through the lucite surface to reach to the MaPMT array. To take the advantage of vertical muon flux we tilted the lucite by  $12^\circ$ . After tilting the lucite we were able to collect the Cherenkov light produced by the muon with an incident angle between 0 to  $6^\circ$  (angular acceptance of muon between the green and vertical black lines) while muon striking from another half (between the black and red lines) were missed due to the total internal reflection and acceptance of the MaPMT array. The trigger was formed by two scintillators S1 and S2, about 5 cm x 5 cm overlapping area, in coincidence. The muon can hit anywhere within the 4 central MaPMTs shown by the red rectangle and form a cluster at the MaPMT array. The expected position of partial (about 35%) Cherenkov ring and muon cluster is shown in Figure 14 (right).

In our setting, we found the good agreement between the observed and expected number of photoelectrons for the background level up to 320 kHz/pixel with both pixel and sum readouts. This suggests that MAROC sum electronics can work as expected up to background similar to SoLID running conditions. To compute the expected number of photoelectrons we took quantum efficiency, partial ring due to total internal reflection, and the transmittance of lucite into account. However, the cosmic rings were not good enough for pattern recognition using Hough transformation. Some of the causes behind the complicated cosmic ring were: use of thick lucite (4 cm), partial ring due to total internal reflection from lucite surface, lack of tracking and optical focusing.

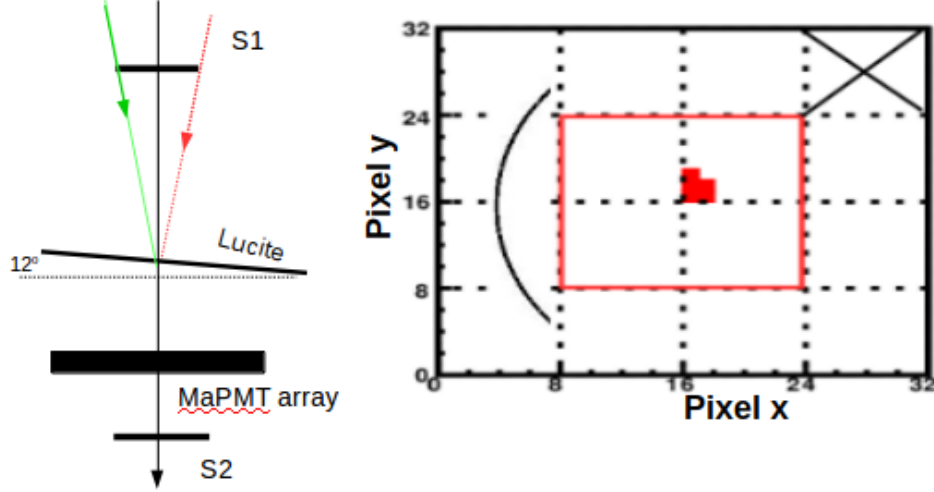


FIG. 14. Left: Schematic layout for the cosmic test. Two scintillators, one at the top and another at bottom of the PMT array form a trigger. Lucite is tilted at an angle  $12^\circ$  with horizontal. The red and the green lines represent the extreme of scintillator acceptance. Due to the total internal reflection and the limited size of the MaPMT array, only about half of the triggered events form the partial ring. Right: The 15 PMTs array of dimension  $\sim 20 \times 20$  cm is used to detect the Cherenkov ring. The cosmic muon can hit any of the central 4 PMTs represented by the red rectangular box.

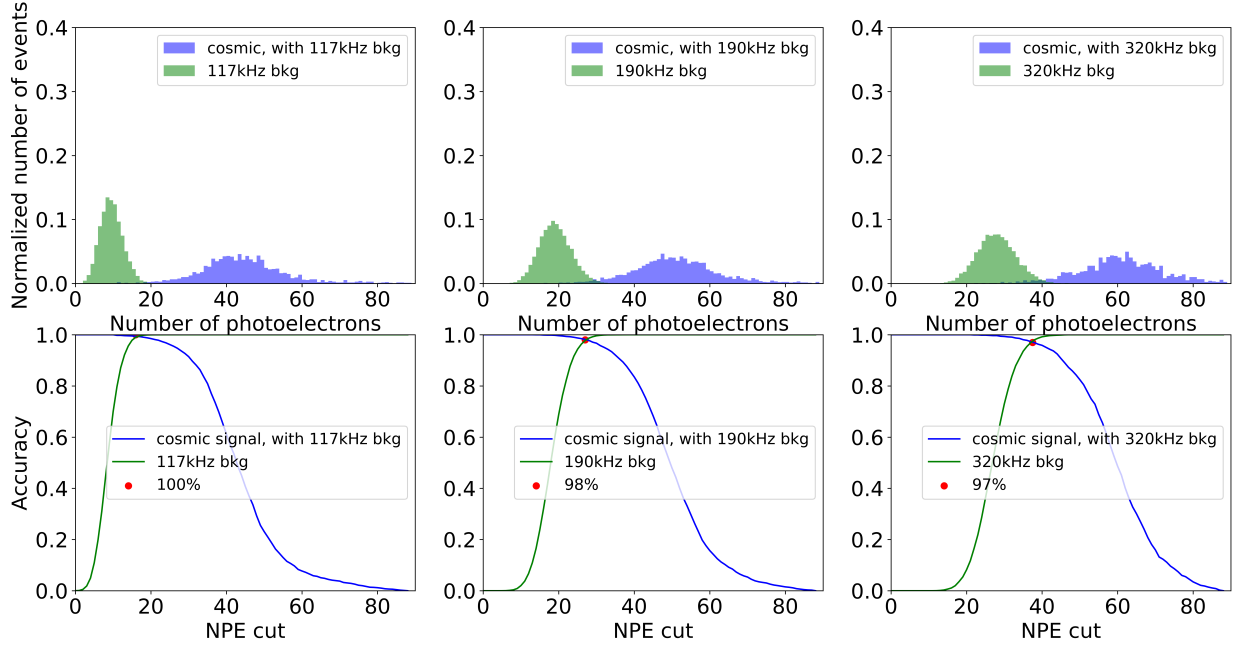


FIG. 15. Top: Number of photoelectron distribution for cosmic data with pixel readout. The green and the purple histogram represents a number of photoelectrons with background only and cosmic in presence of background. The histograms are at the background rate of 117, 190, and 320 kHz/pixel from left to right. Bottom: The figure of merit for the number of photoelectrons cut at different levels of background.

## VI. CONCLUSION

The MAROC sum board can provide analog sum of charge collected in pixel and pixel TDC information simultaneously. MAROC sum board can be one of the potential option to read MaPMT photosensors in the SOLID Cherenkov detector however its performance has not been tested before. We tested some of the features which were importance for SoLID running scenarios at bench using the LED and Laser light source. We found that initial designed had oscillation in FADC signal while multiple boards were operated together. The source of oscillation was coupling of low voltage supply between the boards. With the help of JLab fast electronics group, the sum boards were modified to reduce the pedestal oscillation. We found that above certain input charge the analog sum signal gets saturated. Saturation comes from the summing board. The range of linear regime depends on the number of pixel fired in a group of 8 pixels. Operating at 850 V, the single pixel can hold up to 3 photoelectrons, quadrant can hold 11, and sum can hold 44 photoelectrons before saturation. We also determined that TDC threshold can be set to 30 DAC unit above the mean pedestal of MaPMT while operating at 850 V. While operating at 850 V and TDC threshold 30 DAC unit above mean pedestal we only loose about 5% of signal with low amplitude.

Using pulsed laser and LED operated at DC voltage we exceeded the rate expected in SoLID running condition. We also demonstrated that MAROC electronics performs well up to 6MHz/PMT by studying the linear correlation between the FADC and TDC signal. We analyzed both pixel and sum signal data from the LED produced ring to test simple algorithm, number of photoelectron, cut and some what complicated algorithm, Hough transformation. The number of photoelectron cut was sufficient to discriminate the signal from background below 200 kHz/pixel but above it some complicated algorithm were required. Using Hough transformation, we achieved accuracy above 90% for the background rate up to 370kHz/pixel. For the Cosmic test, we used lucite as radiator. Due to the total internal reflection from lucite surface only able partial ring was observed on MaPMTs array. Good agreement was found between the expected and observed number of photoelectrons in our cosmic setup. Observed cosmic rings were partial, broad without proper tracking, and optical focusing, which made complicated to perform the pattern recognition using the Hough transformation algorithm.

- 
- [1] SoLID Project, Jefferson Lab. <https://solid.jlab.org/>.
  - [2] H. Gao *et al.* Jefferson Lab experiment E12-10-006.
  - [3] H. Gao *et al.* Jefferson Lab experiment E12-11-108.
  - [4] J. Huang *et al.* Jefferson Lab experiment E12-11-007.
  - [5] Z.-E. Meziani *et al.* Jefferson Lab experiment E12-12-006.
  - [6] P. A Souder *et al.* Jefferson Lab experiment E12-10-007.
  - [7] Chao Peng *et al.* Performance of photosensors in high rate environment for gas cherenkov, 2020.
  - [8] Sylvie Blin, Pierre Barrillon, and Christophe de La Taille. MAROC, a generic photomultiplier readout chip. *IEEE Nucl. Sci. Symp. Conf. Rec.*, 2010:1690–1693, 2010.
  - [9] M. Contalbrigo *et al.* The clas12 ring imaging cherenkov detector. *Nuclear Instruments and Methods in Physics Research Section A: Accelerators, Spectrometers, Detectors and Associated Equipment*, 964:163791, 2020.